New 2-pyridinealdehyde *N*⁴-hydroxyethyl thiosemicarbazone and their Cd(II) and Cu(II) complexes: synthesis, spectral, in vitro antibacterial activity and molecular and supramolecular structure study

Reza Takjoo[a]; Mohammad Hakimi[b]; Mohammad Seyyedin[c]; Mozhgan Abrishami[b]

[a] Department of Chemistry, School of Sciences, Ferdowsi University of Mashhad, Mashhad, Iran [b] Department of Chemistry, Payame Noor University (PNU), Mashhad, Iran [c] Department of Quality Control, Razi Vaccine and Serum Research Institute, Mashhad, Iran

PLEASE SCROLL DOWN FOR ARTICLE

Taylor & Francis
Taylor & Francis Group

New 2-pyridinealdehyde N^4-hydroxyethyl thiosemicarbazone and their Cd(II) and Cu(II) complexes: synthesis, spectral, in vitro antibacterial activity and molecular and supramolecular structure study

Reza Takjoo[a]*, Mohammad Hakimi[b], Mohammad Seyyedin[c] and Mozhgan Abrishami[b]

[a]*Department of Chemistry, School of Sciences, Ferdowsi University of Mashhad, Mashhad 91775-1436, Iran;* [b]*Department of Chemistry, Payame Noor University (PNU), Mashhad, Iran;* [c]*Department of Quality Control, Razi Vaccine and Serum Research Institute, Mashhad, Iran*

N^4-hydroxyethyl-pyridinealdehyde thiosemicarbazone (HL, **1**) as a tridentate Schiff base has been synthesized by 1:1 reaction of *S*-methyl-3-((pyridyl)methyl) dithiocarbazate and 2-aminoethanol. Complexes [Cd(HL)$_2$](NO$_3$)$_2$ (**2**), [Cd(HL)I$_2$] (**3**), [Cd(HL)Cl$_2$] (**4**), [Cu(HL)$_2$](NO$_3$)$_2$ (**5**) and [Cu(HL)Cl$_2$] (**6**) have been obtained and characterized by elemental analyses, molar conductivities, and spectroscopic studies. The ligand molecule binds the metal ion using pyridyl nitrogen, azomethine nitrogen and the sulfur atoms. The crystal structure analysis of **3** has been determined and showed to be a distorted square pyramidal geometry complex. The inter- and intramolecular interactions give rise to a supramolecular network. Compounds **2**, **3**, **5** and **6** were assayed for their bioactivities against selected pathogens. Copper(II) complexes **5** and **6** showed antimicrobial activities against Gram-positive (*Bacillus anthracis*) and Gram-negative (*Pseudomonas aeruginosa* and *Yersinia pseudotuberculosis*) bacteria, complexes **2**–**4** showed antimicrobial activities against *Bacillus atrophaeus*, while the ligand itself showed antimicrobial activities against *Escherichia coli* and *Y. pseudotuberculosis*.

Keywords: thiosemicarbazone; transition metal complex; antibacterial activity; crystal structure; supramolecular

1. Introduction

The coordination chemistry of substituted thiosemicarbazones with transition metals has displayed various bonding properties in their complexes and has shown their use in a variety of different applications (*1–3*). The presence of hard N- and soft S-donor atoms in the backbones of these ligands enables them to react readily with both transition and main group metal ions yielding stable metal complexes. Owing to this biological activity, there is a considerable interest in metal complexes of heterocyclic thiosemicarbazones (*4*).

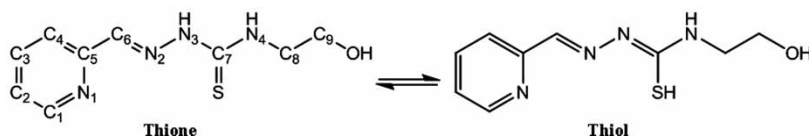*Corresponding author. Email: rezatakjoo@yahoo.com

Figure 1.   Structure of 2-pyridinealdehyde N^4-hydroxyethyl thiosemicarbazone (HL, **1**).

In many cases, the pharmacological activity has been found to be highly dependent on the identity of the metal, chemical nature of the moiety attached to the C=S carbon atom and the donor sequence of the ligands. Furthermore, various ligands widely show different biological activities while their molecular structure may slightly vary; the mechanism is yet to be determined (*5–6*). The development of the pathways that control the architecture of artificial supramolecular systems is one of the major goals in the field of supramolecular chemistry (*7*). In some thiosemicarbazones, there are suitable hydrogen bonds to form supramolecular structures which make them appealing for study. Various columbic and hydrogen interactions between suitable species can create a supramolecular network. The hydrogen bonds between a donor atom couple and an acceptor atom couple in adjacent molecules will increase the probability of the formation of the supramolecular network. Although generally considered weak, the hydrogen bonding involving the sulfur atom takes a significant place among the stabilizing factors (*8*).

In the work reported here, the new tridentate thiosemicarbazone ligand *N*-(2-hydroxyethyl)-2-(pyridin-2-ylmethylene)hydrazinecarbothioamide (HL, **1**) (Figure 1) and its Cd(II) and Cu(II) complexes have been synthesized. The HL molecule is designed as two parts. The first part hydroxyethyl increases the supramolecular formation by providing hydrogen bonds. The second part, pyridyl ring, is selected according to its expected biological activities.

These compounds were characterized by ^{1}H NMR, ^{13}C NMR, Infrared (IR), UV–VIS, and carbon hydrogen nitrogen sulfur (CHNS) analyses. The structure of [Cd(HL)I$_2$] (**3**) complex has been determined by X-ray crystallography. Furthermore, the biological activities of a set of synthesized thiosemicarbazones compounds against a panel of Gram-positive bacteria including *Staphylococcus aureus*, *Bacillus anthracis* and *Bacillus atrophaeus* and Gram-negative bacteria including *Yersinia pseudotuberculosis*, *Escherichia coli* and *Pseudomonas aeruginosa* have been studied.

2.   Results and discussion

The thiosemicarbazone ligand and complexes were prepared as described in Section 4. *N*-(2-hydroxyethyl)-2-(pyridin-2-ylmethylene)hydrazinecarbothioamide (HL, **1**) like most thiosemi-carbazones can exhibit thione–thiol tautomerism (Figure 1).

HL interacts with metal ions in a molar ratio of 2:1 or 1:1, in the presence of appropriate anions, yielding complexes with the empirical formula of [Cd(HL)$_2$](NO$_3$)$_2$ (**2**), [Cd(HL)I$_2$] (**3**), [Cd(HL)Cl$_2$] (**4**), [Cu(HL)$_2$](NO$_3$)$_2$ (**5**) and [Cu(HL)Cl$_2$] (**6**). This tridentate ligand acts as a thione form in all complexes. The color, yield, molar conductance and elemental analysis data of all the complexes are presented in Section 4. All of the compounds are stable in air and can be kept in a desiccator for a long time without any signs of decomposition. The molar conductivities of 10^{-3} M solutions in dimethylformamide (DMF) of the complexes indicate that the molar conductance of compounds **3**, **4** and **6** falls well below the value expected for a 1:1 electrolyte and they are non-electrolytes. Conductivity data for **2** and **5** point to their electrolytic nature. According to the reports of similar structures (*9–15*) and following results, compounds **2** and **5** have a distorted octahedral geometry and the other complexes have a distorted square pyramidal geometry.

2.1. *IR spectra*

The IR spectra of the free ligand and metal complexes were studied and assigned based on their comparison. The assignments of main IR bands of the compounds in 400–4000 cm^{-1} region are presented in Section 4. The strong bands at 3222 and 3151 cm^{-1} in the spectra of the ligand have been assigned to $\nu(^4N-H)$ and $\nu(^3N-H)$, respectively (Figure 1).

In the complexes, the stretching bond of $\nu(^4N-H)$ shift to both higher and lower energies, suggesting differences in hydrogen bonding of ^{4}NH between the uncomplexed and complexed thiosemicarbazone (*16*). The ligand displays no band at ca. 2800–2550 cm^{-1} region associated with $\nu(S-H)$ (*17*), indicating that it exists in the thione form in the solid state. The out-of-plane bending vibrations of the pyridine ring at 634 cm^{-1} in the spectrum of **1** are shifted on complexation, suggesting the coordination of the ligand to the metal ions via the pyridine nitrogen (*18*). A strong band at 1068 cm^{-1} in the compound **1** is assigned to the $\nu(N-N)$ vibration which is observed in the range of 1074–1047 cm^{-1} after coordination (*19*). In the spectrum of the free base **1**, the absorption at ca. 879 cm^{-1} is attributed to the $\delta(CS)$ vibration, and in the spectra of the complexes it shifts to lower frequencies (823–777 cm^{-1}). This indicates the coordination via the sulfur atom (*20, 21*). Furthermore, the $\nu(C=S)$ stretching vibration is observed as a band at 1365 cm^{-1} in compound **1** which reveals a negative shift after complexation (*22*). In the complexes, the band around 1383 cm^{-1} is attributed to D_{3h} mode of the free NO_3^- group which is not involved in coordination, suggesting the uncoordination of nitrate groups as counter-ions (*23*). Finally, the broad band at 3445–3390 cm^{-1} is assigned to the $-$OH moiety stretching.

2.2. *Nuclear magnetic resonance studies*

The ^{1}H NMR is a useful method for the identification of organic and diamagnetic compounds with the help of other spectrometric data. The spectra of **1** and some metal complexes were carried out in DMSO-d_6 because this is the only solvent which dissolves all the above compounds. The chief ^{1}H NMR data discussed based on the atom labeling in Figure 1 are listed in Section 4.

A sharp singlet signal at $\delta = 11.70$ ppm in the ^{1}H NMR spectrum of uncomplexed thiosemi-carbazone is attributed to ^{3}NH. This proton shows a downfield shift due to the decreases in the electron density of proton in the intra- or intermolecular hydrogen-bonding interaction in the solvent, suggesting *Z*-form configuration in the solution (*24*). A triplet is centered at 4.80 ppm which can be assigned to the proton of the nitrogen atom ^{4}N. The resonance splits as a triplet due to quadrupole splitting (*17*). The signals of ^{3}NH, ^{4}NH and OH peaks disappear by the addition of D_2O, suggesting that they are easily exchangeable.

For pyridyl ring, a doublet at $\delta = 8.55$ ppm is assigned to the ^{1}CH proton. The presence of the electronic effect of the adjacent electronegative pyridyl nitrogen shifts ^{1}CH proton to downfield. ^{2}CH is coupled with ^{1}CH and results in forming a doublet. ^{3}CH, ^{2}CH and ^{4}CH are found in 8.15, 7.83, and 7.35 ppm, respectively, and all are triplets. The methine proton ^{6}CH is observed at 8.1 ppm as a singlet. The absence of any peak around 1.6–2.2 ppm corresponding to the SH proton in **1** indicates that the ligand is present in the thione form in solution (*2*).

The ^{1}H NMR spectra of the complexes are less resolved than those of the ligand, perhaps due to the low solubility of the complexes (*17*). Thus, these spectra show that the resonance peaks are shifted from their corresponding values in the ligand as a result of coordination. The existence of the ^{3}NH resonance in the ^{1}H NMR spectra of complexes indicates that the nitrogen atoms remain as protonated and HL coordinates as neutral ligand. The pyridyl ring signals after coordination exhibit a low intensity of the multiplets that may be attributed to the delocalization of electron density due to coordination in the complex. The ^{1}CH signal (at 8.5 ppm in HL) shifts downfield in complexes because coordination through the pyridine nitrogen atom prevents ^{1}CH from being deshielded, as it is in the free ligand, due to the anisotropy of the C(6) $=$ N(2) bond and the

proximity of the sp^2 nitrogen (*25*). However, protons in CH_2CH_2OH, which do not take part in coordination, remain more or less unchanged in the complexes. There are perhaps slight variations in their resonances due to the delocalization of electron density in the system.

2.3. *Electronic spectra*

The assignments of the significant electronic spectral bands of the ligand and its complexes are presented in Section 4. Electronic spectra were obtained in DMF solution.

The electronic spectrum in the methanol solution of HL shows two bands corresponding to n → π* transition of the pyridyl ring which is observed at 274 nm; however, the n → π* transition of azomethine and thioamide functions of the thiosemicarbazone moiety are observed at 324 nm, in which both the latter moieties overlap under the same envelop (*26*). Furthermore, the molar absorptivity for n → π* transitions for the solution spectrum is $> 10^4$, which is consistent with the previously studied heterocyclic thiosemicarbazones (*27*). In the electronic spectra of the complexes, the n → π* transitions are shifted as a result of coordination. The electronic spectra of complexes show n → π* transitions at 383–245 nm. The band in the range of 420–409 nm observed in the spectra is assigned to ligand to metal charge transfer (LMCT) (S → Cu and py → Cu) transition. For all colored complex solutions, we expect to observe bands at visible regions. The d–d transitions occur at much lower energy regions and are weak in nature. The broad CT band, tailing into the visible region, causes to hide some weak d → d transitions in Cu complexes and only one d–d transition is observed at 626 and 607 nm for compounds **5** and **6**, respectively. The absence of d → d band in Cd complexes spectra is relevant to the d^{10} configuration of Cd^{II} (*28*).

2.4. *Crystal structure*

The oak ridge thermal ellipsoid plot (ORTEP) diagram of the [Cd(HL)I$_2$] molecule with its atom numbering scheme is shown in Figure 2. Selected bond lengths and bond angles are given in
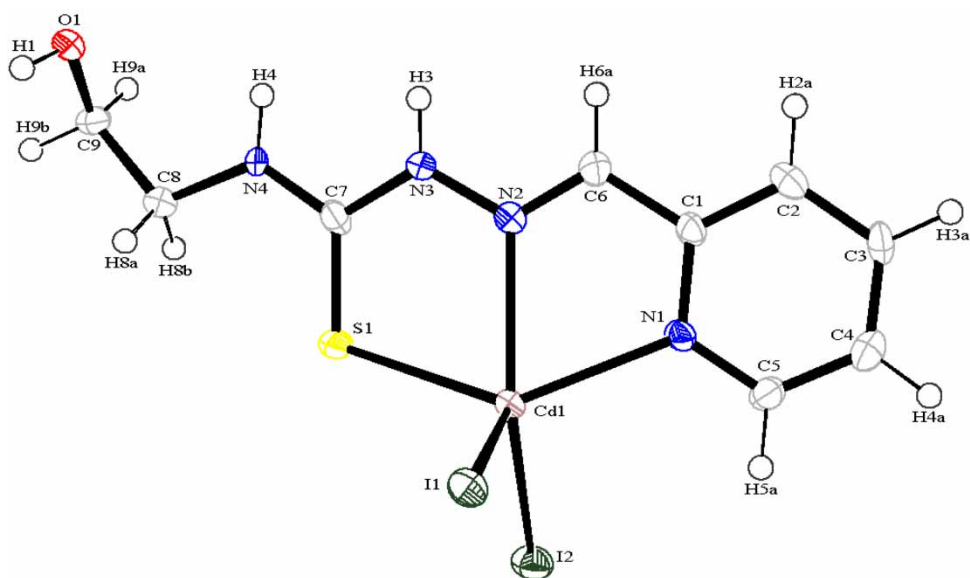

Figure 2.   Molecular plot of [Cd(HL)I$_2$] (**3**) with the thermal ellipsoids representing 50% probability.

Table 1. Bond lengths (Å) and angles (°) for **3**.

Cd(1)–I(2)	2.7805(9)	I(1)–Cd(1)–I(2)	108.74(3)
Cd(1)–I(1)	2.7443(8)	N(1)–Cd(1)–N(2)	68.1(2)
Cd(1)–S(1)	2.620(2)	N(2)–Cd(1)–S(1)	72.09(17)
Cd(1)–N(2)	2.399(6)	S(1)–Cd(1)–I(2)	95.50(5)
Cd(1)–N(1)	2.356(6)	N(1)–Cd(1)–I(2)	102.42(16)
N(4)–C(8)	1.460(10)	N(1)–Cd(1)–I(1)	104.96(16)
N(3)–C(7)	1.368(10)	S(1)–Cd(1)–I(1)	106.55(5)
N(1)–C(1)	1.367(10)	N2–Cd(1)–I(1)	112.34(16)
N(2)–N(3)	1.350(9)	N(1)–Cd(1)–S(1)	136.14(17)
N(1)–C(5)	1.328(10)	N(2)–Cd(1)–I(2)	138.91(16)
N(4)–C(7)	1.300(10)	C(1)–N(1)–Cd(1)	117.4(5)
N(2)–C(6)	1.267(10)	C(5)–N(1)–C(1)	118.0(7)
O(1)–C(9)	1.419(10)	C(6)–N(2)–Cd(1)	119.1(6)
S(1)–C(7)	1.696(8)	N(2)–N(3)–C(7)	120.0(7)
C(8)–C(9)	1.497(11)	C(6)–N(2)–N(3)	120.1(7)
C(1)–C(6)	1.459(11)	N(3)–N(2)–Cd(1)	120.4(5)
C(2)–C(3)	1.392(12)	C(7)–N(4)–C(8)	123.9(7)
C(4)–C(5)	1.388(11)	C(5)–N(1)–Cd(1)	124.1(5)
C(1)–C(2)	1.387(11)	C(7)–S(1)–Cd(1)	101.7(3)
C(3)–C(4)	1.368(11)	N(4)–C(8)–C(9)	110.8(6)
		O(1)–C(9)–C(8)	112.2(7)
		N(4)–C(7)–N(3)	115.7(7)
		N(1)–C(1)–C(6)	116.6(7)
		N(2)–C(6)–C(1)	117.8(7)
		C(4)–C(3)–C(2)	118.1(7)
		C(1)–C(2)–C(3)	119.2(8)
		C(3)–C(4)–C(5)	120.2(8)
		C(2)–C(1)–C(6)	121.5(7)
		N(1)–C(1)–C(2)	121.9(8)
		N(4)–C(7)–S(1)	122.1(6)
		N(3)–C(7)–S(1)	122.1(6)
		N(1)–C(5)–C(4)	122.5(8)

Table 1. The compound crystallized with one monomer per asymmetric unit into triclinic crystal system with a space group $P\bar{1}$. The structure shows that the complex is a monomer in which the Cd(II) atom adopts a five-coordinate geometry with the neutral Schiff base being coordinated to it as a tridentate chelating agent via the pyridyl nitrogen atom (N(1)), the azomethine nitrogen atom (N(2)), the thione sulfur atom (S(1)) and two iodine atoms.

This five-coordinate geometry can adopt either a square pyramidal or a trigonal bipyramidal structure. To determine such structures, the formula of Addison *et al.* (*29*) is applied in which the angular structural parameter (τ) is represented as the index of trigonality. The parameter $\tau = \beta - \alpha/60$, where α and β are the two largest angles, belongs to the cadmium atom. An ideal square pyramid will have $\beta = 180°$ and $\alpha = 180°$, and therefore $\tau = 0\%$, but an ideal trigonal bipyramidal structure will have $\beta = 180°$ and $\alpha = 120°$ and therefore $\tau = 100\%$. The τ-value is calculated to be 4.62%, indicating the slightly distorted square pyramidal geometry around Cd(II) ion.

The donor atoms of thiosemicarbazone (N(1), N(2), and S(1)) together with an iodine atom (I(2)) form the basal plane of the square pyramid and the other iodine atom (I(1)) occupies the apical position. The molecule exists in the *Z* conformation with respect to the C(6)–N(2) bond and the S(1) and N(2) atoms are in the *E* conformation with respect to the N(3)–C(7) bond; hence, the thiosemicarbazone moiety, as a whole, exists in the *ZE* conformation. This conformation may be due to the steric effects of the ligand and is not attributed to electronic effects because Cd(II), as a metal center, has d^{10} configuration and does not feel the ligand field stabilization effects.

The C(6)–N(2) (1.267(10) Å) and C(7)–S(1) (1.696(8) Å) bond distances are indicative of a considerable double bond character. Cd–N_{py} (2.356(6) Å) distance in this complex is shorter than

Cd–N$_{imine}$ (2.399(6) Å) distance, whereas the azomethine nitrogen atom is typically a stronger donor than that of pyridine. This observation can be found in some kind of Cd complexes (*9*). The two Cd–I distances are different and their discrepancy (0.04 Å) is bigger than that of [Cd(HAm4DH)I$_2$] (0.002 Å) (*10*).

The angle between root mean square (rms) planes of thiosemicarbazone moiety and I(2)–Cd(1)–I(1) is about 2.6°, which indicates that these planes are nearly perpendicular. In this case, the steric effect causes an angle difference (6.71°) between the two rms planes of thiosemicarbazone moiety and pyridyl ring. This angle value is smaller and bigger than that of [Cd(HAm4DH)I$_2$] and [Cd(HAm4E)I$_2$], respectively (*15*).

Furthermore, comparative X-ray structure of **1** with similar compounds demonstrates that Cd(1)–I(1) distance is shorter and Cd(1)–S(1) and Cd(1)–N(2) are longer in **1** than that of the others ([Cd(HAm4DH)I$_2$], [Cd(HAm4DH)I$_2$] and [Cd(HAm4E)I$_2$]).

The hydrogen bonds and other intermolecular interactions play an important role in this compound lattice. The presence of appropriate donor and acceptor atoms in the molecule gives rise to the formation of supramolecular. The hydrogen bonds N(3)–H(3)··· O(1) and N(4)–H(4)··· O(1) joint two molecules which form a dimer (Figure 3). These dimers are connected to each other via O(1)–H(1)··· I(2) hydrogen bond, causing the expansion of crystal chain growth in one dimension along [1,−1,0] vector (Figure 4). Hydrogen bond parameters are given in Table 2.
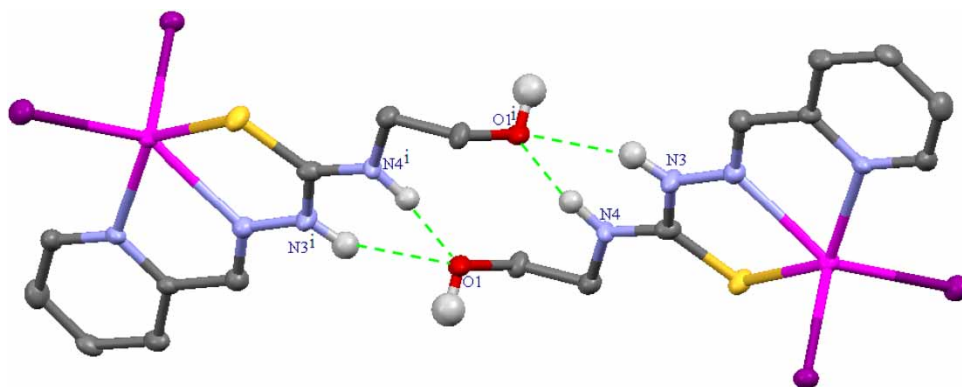

Figure 3.   Intermolecular hydrogen bonds in dimer formation (symmetry position i: −*x*, 2 − *y*, 2 − *z*).
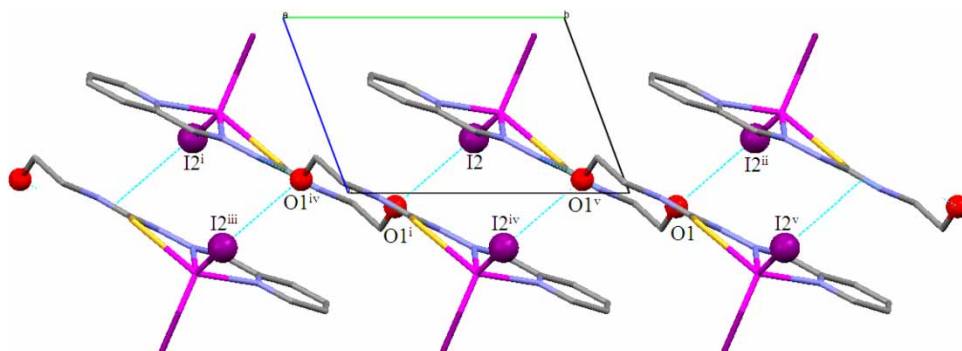

Figure 4.   The effect of O1–H1··· I2 interactions in 1D development (symmetry position i: 1 + *x*, −1 + *y*, *z*; ii: −1 + *x*, 1 + *y*, *z*; iii: 2 + *x*, −*y*, 2 − *z*; iv: 1 − *x*, 1 − *y*, 2 − *z*; v: −*x*, 2 − *y*, 2 − *z*).

Table 2. Hydrogen bonds for **3**.

D–H···A	d(D–H)	d(H···A)	d(D···A)	<(DHA)
O(1)–H(1)···I(2)#^{a}1	0.84	2.64	3.404(6)	152
N(3)–H(3)···O(1)#2	0.88	2.15	2.922(11)	147
N(4)–H(4)···O(1)#2	0.88	2.03	2.848(10)	155

Note: ^{a}Symmetry transformations used to generate equivalent atoms: #1: $x - 1, y + 1, z$; #2: $-x, -y + 2, -z + 2$.

Table 3. Agar disk diffusion test (diameter of growth inhibitory zone by mm).

Compound	Gram-positive bacteria			Gram-negative bacteria		
	B. atrophaeus	*S. aureus*	*B. anthracis*	*P. aeruginosa*	*E. coli*	*Y. pseudotuberculosis*
HL (**1**)	11	0	13	10	10	15
[Cd(HL)](NO$_3$)$_2$ (**2**)	24	18	17	0	0	0
[Cd(HL)I$_2$] (**3**)	20	17	18	0	0	0
[Cd(HL)Cl$_2$] (**4**)	23	20	22	0	0	0
Cd(NO$_3$)$_2$	17	10	0	0	0	0
[Cu(HL)$_2$](NO$_3$)$_2$ (**5**)	16	18	24	0	0	0
[Cu(HL)Cl$_2$] (**6**)	11	17	22	17	10	10
Cu(NO$_3$)$_2$	0	0	0	0	0	0

2.5. *Antimicrobial activity study*

The thiosemicarbazone (TSC) (**1**) and its complexes have been tested for *in vitro* inhibitory activity against the growth of several selected pathogens to evaluate their antibacterial properties. For tetracycline and streptomycin with a concentration of 1.5 mg/disk, $d \geq 20$ mm, $14 \leq d < 20$ mm, and $9 \leq d \leq 13$ mm show high, moderate and slight sensitivities, respectively (*30*). As the results collected in Table 3 indicate, the complexes are intermediately to strongly active against Gram-positive bacteria and have a weak activity against Gram-negative bacteria (except **6** which has an intermediate activity against *P. aeruginosa*).

The results of disc diffusion method studies given in Table 3 indicate that only compounds **1** and **6** are active against Gram-negative bacteria. The data of quantitative antimicrobial analyses in Table 4 (minimum inhibitory concentration (MIC), minimum bactericidal concentration (MBC)) show that metal complexes have generally better antibacterial activity against Gram-positive bacteria than that of the free ligand and metal nitrate salts. It seems that the antibacterial activities of the ligand are significantly enhanced by their chelation to the metal. Compound **3** does not show any activity against the organism *P. aeruginosa*. In Gram-positive bacteria, the Cu complexes have a robust activity against *B. anthracis*, while Cd complexes are strongly active against *B. atrophaeus* and *B. anthracis*. In Gram-negative bacteria, the free ligand (**1**) possesses a good antibacterial activity, especially against *E. coli* and *Y. pseudotuberculosis*, perhaps due to its less hydrophilic property and therefore its better passage across the cell wall. Moreover, compound **6** shows a good inhibition against *Y. pseudotuberculosis*. The results obtained from nitrate salts tests indicate that in comparison with metal complexes, the nitrate ions do not have any significant antibacterial activity.

3. Conclusion

We have prepared a new nitrogen nitrogen sulfur (NNS) Schiff base HL along with its Cd(II) and Cu(II) complexes.

In the complexes, the ligand acts as a neutral-charged tridentate coordinated to the bivalent metal ion via the pyridyl nitrogen, the azomethine nitrogen and thione sulfur atoms. The geometry

Table 4.   Minimum inhibitory concentration (MIC) and minimum bactericidal concentration (MBC) tests by µg/µL.

| Compound | Gram-positive bacteria | | | | | | Gram-negative bacteria | | | | | |
| | *B. atrophaeus* | | *S. aureus* | | *B. anthracis* | | *P. aeruginosa* | | *E. coli* | | *Y. pseudotuberculosis* | |
	MIC	MBC	MIC	MBC	MIC	MBC	MIC	MBC	MIC	MBC	MIC	MBC
HL (**1**)	0.25	1	2	G[a]	0.125	0.25	1	4	0.125	1	0.125	0.5
[Cd(HL)$_2$](NO$_3$)$_2$ (**2**)	0.0625	0.0625	0.5	2	0.0625	0.125	4	G	2	G	1	G
[Cd(HL)I$_2$] (**3**)	0.0625	0.0625	1	2	0.0625	0.125	4	G	2	G	1	G
[Cd(HL)Cl$_2$] (**4**)	0.0625	0.0625	1	2	0.0625	0.125	4	G	2	G	1	G
Cd(NO$_3$)$_2$	0.5	2	1	4	0.0625	0.25	4	G	4	G	2	G
[Cu(HL)$_2$](NO$_3$)$_2$ (**5**)	0.125	0.25	0.25	0.5	0.0625	0.0625	2	4	1	2	1	2
[Cu(HL)Cl$_2$] (**6**)	0.25	0.5	0.125	0.25	0.0625	0.0625	1	2	1	2	0.25	1
Cu(NO$_3$)$_2$	0.25	1	2	2	0.5	1	2	4	1	2	1	2

Note: [a]G: growth.

around the central metal in compounds **2** and **5** is distorted octahedral and the others have distorted square pyramidal geometries.

An X-ray crystal structure determination of [Cd(HL)I₂] confirms a distorted square pyramidal geometry. Although metal complexes are effective against Gram-positive bacteria (Cu complexes against *B. anthracis* and Cd complexes against *B. atrophaeus* and *B. anthracis*), the free ligand is effective against Gram-negative bacteria (*E. coli* and *Y. pseudotuberculosis*).

4. Experimental

4.1. *Materials and techniques*

All chemicals of AR grade for the synthesis of the thiosemicarbazone ligand and their complexes were used as received.

C, H, N, and S analyses were obtained with a Thermo Finnigan Flash Elemental Analyzer, model 1112EA. IR spectra were recorded from KBr pellets in the range of 4000–400 cm^{-1} on an FT-IR 8400-SHIMADZU spectrophotometer. ^{1}H NMR spectra were recorded on a Bruker BRX 100 AVANCE operating at the frequency of 100 MHz and using DMSO-d_6 and TMS as the solvent and the internal standard with $\delta = 0$, respectively. The ^{13}C NMR spectrum of HL was recorded on a Bruker BRX-300 AVANCE. Electronic spectra of the complexes in DMF solution (ca. 25°C) were recorded by a spectrophotometer SHIMADZU model 2550 UV–VIS spectrophotometer (250–900 nm). Melting points were determined with a Barnsted Electrothermal 9200 electrically heated apparatus.

4.2. *Synthesis of the ligand (HL, 1)*

S-methyl dithiocarbazate was prepared using a reported procedure (*31*). Preparation of *S*-methyl-3-((pyridyl)methyl)dithiocarbazate: a solution of *S*-methyl dithiocarbazate (1.2 g, 1 mmol) in hot ethanol (10 mL) was treated with pyridine 2-carbaldehyde (0.1 ml, 1 mmol) and the resultant mixture was heated on a steam bath for 20 min. The solution was allowed to cool and the fine yellowish needles of the compound separated out. It was filtered off, washed with cold ethanol and dried over silica gel.

HL was prepared by refluxing an ethanolic solution of a 1:1 *S*-methyl-3-((pyridyl)methyl) dithiocarbazate with excess amounts of 2-aminoethanol for ca. 24 h at water bath temperature (until moistened lead nitrate paper indicated that the evolution of methyl mercaptan had stopped). The warm solution was filtered; the resulting yellow solid was washed with MeOH and dried *in vacuo* over silica gel at room temperature.

HL (**1**): yellow, Yield: 47%. m.p.: 198°C. Anal. Calcd for C₉H₁₂N₄OS (224.28 g mol^{-1}): C, 48.20; H, 5.39; N, 24.98; S, 14.30. Found: C, 48.19; H, 5.42; N, 27.61; S, 14.16%. IR spectrum in KBr, cm^{-1}: ν(NH) 3223, 3152m, ν(C=N) +ν(C=C) +δ(N−H) 1539s, ν(C=S) 1298m, ν(C−O) 1221m, ν(N−N) 1070m, δ(C=S) 927w, ρ(py) 634w. UV/VIS (CH₃OH), λ_{max}, nm (log ε, L mol^{-1} cm^{-1}): 211 (3.72), 232 (3.43), 276 (3.46), 324 (4.04). UV/VIS (DMF), λ_{max}, nm (log ε, L mol^{-1} cm^{-1}): 276 (3.61), 324 (4.22). ^{1}H NMR (100 MHz, DMSO-d_6): $\delta = 11.71$ (s, 1H, N³H; exchanges with D₂O) 8.52 (d, 1H, CH=N) 8.55 (d, 1H, C$_{py}^1$) 8.53 (t, 1H, C$_{py}^3$) 7.83 (t, 1H, C$_{py}^2$) 7.35 (t, 1H, C$_{py}^4$) 4.80 (s, br, 1H, N⁴H; exchanges with D₂O) 3.60 (s, 5H, CH₂CH₂OH; OH exchanges with D₂O). ^{13}C NMR (300 MHz, DMSO-d_6): $\delta = 46.511$ (C⁸), 59.615 (C⁹), 120.552 (C⁴), 124.554 (C²), 136.975 (C³), 142.704 (C¹), 149.836 (C⁶), 153.667 (C⁵), 177.840 (C⁷).

The structure of the ligand is given in Figure 1.

4.3. *Synthesis of complexes*

The complexes were prepared by the following procedure. A solution of HL (1 or 2 mmol) in ethanol (10 mL) was added to a solution of appropriate metal salts (1 mmol) in 10 mL of ethanol, and the mixture was refluxed for 3–6 h. The resulting solids were filtered off, washed with cold ethanol and dried over silica gel.

[Cd(HL)$_2$](NO$_3$)$_2$ (**2**): yellow, Yield: 60%. m.p.: 152°C. Molar conductivity (1×10^{-3} mol L^{-1}; DMF): 103.6 Ω^{-1} cm^2 mol^{-1}. Anal. Calcd for C$_{18}$H$_{24}$CdN$_{10}$O$_8$S$_2$ (682.97 g mol^{-1}): C, 30.75; H, 3.73; N, 19.92; S, 9.12. Found: C, 30.90; H, 3.51; N, 20.18; S, 8.94%. IR spectrum in KBr, cm^{-1}: ν(OH) 3402m, ν(NH) 3222m, ν(C=N)+ν(C=C)+δ(N−H) 1583s, ν(NO$_3$) 1381s, ν(C=S) 1319m, ν(C−O) 1240m, ν(N−N) 1074m, δ(C=S) 929w, ρ(py) 646w. UV/VIS (DMF), λ_{max}, nm (log ε, L mol^{-1} cm^{-1}): 292 (3.97), 396 (4.03). ^{1}H NMR (100 MHz, DMSO-d_6): δ = 11.8 (s, 1H, N^{3}H; exchanges with D$_2$O), 8.2 (s, 1H, CH=N), 7.4–8.5 (m, 4H, CH$_{py}$), 4.80 (s, br, 1H, N^{4}H; exchanges with D$_2$O), 3.51 (s, 5H, CH$_2$CH$_2$OH; OH exchanges with D$_2$O).

[Cd(HL)I$_2$] (**3**): yellow, Yield: 75%. m.p.: 242°C. Molar conductivity (1×10^{-3} mol L^{-1}; DMF): 19.70 Ω^{-1} cm^2 mol^{-1}. Anal. Calcd for C$_9$H$_{12}$CdI$_2$N$_4$OS (590.50 g mol^{-1}): C, 18.34; H, 1.88; N, 9.50; S, 5.44. Found: C, 18.37; H, 1.98; N, 10.17; S, 5.27%. IR spectrum in KBr, cm^{-1}: ν(OH) 3433m, ν(NH) 3248, 3053m, ν(C=N)+ν(C=C)+δ(N−H) 1564s, ν(C=S) 1273m, ν(C−O) 1234m, ν(N−N) 1047m, δ(C=S) 920w, ρ(py) 687w. UV/VIS (DMF), λ_{max}, nm (log ε, L mol^{-1} cm^{-1}): 322 (4.41), 396 (4.31). ^{1}H NMR (100 MHz, DMSO-d_6): δ = 11.8 (s, 1H, N^{3}H; exchanges with D$_2$O), 8.7 (s, 1H, CH=N), 7.8–8.6 (m, 4H, CH$_{py}$), 4.70 (s, br, 1H, N^{4}H; exchanges with D$_2$O), 3.60 (s, 5H, CH$_2$CH$_2$OH; OH exchanges with D$_2$O). Crystals suitable for X-ray data collection were obtained from DMF.

[Cd(HL)Cl$_2$] (**4**): yellow, Yield: 78%. m.p.: 231.5°C. Molar conductivity (1×10^{-3} mol L^{-1}; DMF): 20.47 Ω^{-1} cm^2 mol^{-1}. Anal. Calcd for C$_9$H$_{12}$CdCl$_2$N$_4$OS (407.60 g mol^{-1}): C, 30.75; H, 3.73; N, 19.92; S, 9.12. Found: C, 30.75; H, 3.51; N, 20.18; S, 8.94%. IR spectrum in KBr, cm^{-1}: ν(OH) 3445m, ν(NH) 3213, 3022m, ν(C=N)+ν(C=C)+δ(N−H) 1564s, ν(C=S) 1300m, ν(C−O) 1242m, ν(N−N) 1068m, δ(C=S) 899w, ρ(py) 631w. UV/VIS (DMF), λ_{max}, nm (log ε, L mol^{-1} cm^{-1}): 322 (4.39), 396 (4.21). ^{1}H NMR (100 MHz, DMSO-d_6): δ = 11.8 (s, 1H, N^{3}H; exchanges with D$_2$O), 8.54 (s, 1H, CH=N), 7.4–8.58 (m, 4H, CH$_{py}$), 4.50 (s, br, 1H, N^{4}H; exchanges with D$_2$O), 3.57 (s, 5H, CH$_2$CH$_2$OH; OH exchanges with D$_2$O).

[Cu(HL)$_2$](NO$_3$)$_2$ (**5**): green, Yield: 43.5%. m.p.: 159°C. Molar conductivity (1×10^{-3} mol L^{-1}; DMF): 114.5 Ω^{-1} cm^2 mol^{-1}. Anal. Calcd for C$_{18}$H$_{24}$CuN$_{10}$O$_8$S$_2$ (636.12 g mol^{-1}): C, 33.99; H, 3.80; N, 22.02; S, 10.08. Found: C, 30.64; H, 3.91; N, 23.22; S, 9.70%. IR spectrum in KBr, cm^{-1}: ν(OH) 3390m, ν(NH) 3327, 3269m, ν(C=N) 1612s, ν(N=C) 1529s, ν(C=S) 1296m, ν(C−O) 1234m, ν(N−N) 1055m, δ(C=S) 925w, δ(NO$_3$) 887w, ρ(py) 623w. UV/VIS (DMF), λ_{max}, nm (log ε, L mol^{-1} cm^{-1}): 323 (4.35), 409 (3.81), 623 (1.93).

[Cu(HL)Cl$_2$] (**6**): green, Yield: 88%. m.p.: 222°C. Molar conductivity (1×10^{-3} mol L^{-1}; DMF): 49.64 Ω^{-1} cm^2 mol^{-1}. Anal. Calcd for C$_9$H$_{12}$Cl$_2$CuN$_4$OS (358.73 g mol^{-1}): C, 30.13; H, 3.37; N, 15.62; S, 8.94. Found: C, 30.17; H, 3.42; N, 15.59; S, 9.03%. IR spectrum in KBr, cm^{-1}: ν(OH) 3402m, ν(NH) 3335, 3202m, ν(C=N)+ν(C=C)+δ(N−H) 1591s, ν(C=S) 1308m, ν(C−O) 1238m, ν(N−N) 1057m, δ(C=S) 939w, ρ(py) 634w. UV/VIS (DMF), λ_{max}, nm (log ε, L mol^{-1} cm^{-1}): 298 (4.1), 343 (3.9), 420 (3.9), 607 (2.12).

4.4. *Qualitative and quantitative antimicrobial activity*

The free ligand and the complexes were tested for antimicrobial activity. Six pathogenic bacteria were used to test the antibacterial potentials of the thiosemicarbazone and its complexes.

The organisms chosen for antimicrobial activity were three Gram-positive (*S. aureus*, *B. anthracis* and *B. atrophaeus*) and three Gram-negative (*Y. pseudotuberculosis*, *E. coli* and

P. aeruginosa) bacteria. The antimicrobial activity of all compounds was screened qualitatively by a modified disc diffusion method (*6*). Agar disc diffusion method was carried out using brain heart agar media and 6 mm diameter paper discs of Whatman filter paper No. 1. The compounds were dissolved in DMSO to give a concentration of ca. 1.5 µg/disc. One of the media was cultured with Swab (sterile, nontoxic) containing 1:10 dilution of 0.5 McFarland suspensions of bacterial broth media (10^7 CFU/mL). The plates were incubated at 35°C for 24 h, and the inhibition zone around each disc was measured.

All the Compounds were subjected to the broth dilution method for the quantitative measurement of bacteriostatic (MIC) and bacteriocidal (MBC) activities. The lowest concentration, in which visible microbial growth was completely inhibited, was recorded as the MIC (µg/µL). The simplest method for determining the MBC is to perform a subculture from antibiotic concentrations with no visible growth in the MIC (µg/µL) test onto antibiotic-free agar. This will determine whether the bacteria are growth-inhibited but still viable or they are killed.

4.5. *Crystal structure solution*

An appropriate yellow prism-shaped single crystal of **3**, with approximate dimensions of 0.25 × 0.25 × 0.12 mm, was mounted on a glass fiber and intensity data were measured at 100(2) K. The unit cell parameters and the intensity data were collected on a Bruker APEX-II CCD diffractometer using graphite monochromated Mo-Kα radiation (0.71073 Å) with φ- and ω-scan techniques.

The software SMART and SAINTPlus were applied for data acquisition and data abstraction, respectively. Absorptions corrections on the data were made using SADABS (*32*). The structure was solved by direct methods (*33*) and refined by full-matrix least squares based on F^2 with weight

Table 5. Crystal data and structure determination details for **3**.

Compound	**3**
Empirical formula	$C_9H_{12}CdI_2N_4OS$
Formula weight	590.49
Temperature	100(2) K
Wavelength	0.71073 Å
Crystal system	Triclinic
Space group	$P\bar{1}$
Unit cell dimensions	$a = 9.6129(11)$ Å, $\alpha = 64.313(2)°$
	$b = 9.7288(12)$ Å, $\beta = 66.973(2)°$
	$c = 10.2245(12)$ Å, $\gamma = 70.289(2)°$
Volume	776.67(16) Å^3
Z	2
Density (calculated)	2.525 Mg/m^3
Absorption coefficient	5.509 mm^{-1}
$F(000)$	544
Crystal size	0.25 × 0.25 × 0.12 mm^3
Theta range for data collection	2.31–29.00°
Index ranges	$-13 <= h <= 13, -13 <= k <= 13, -13 <= l <= 13$
Reflections collected	9024
Independent reflections	4082 [$R_{(int)} = 0.0665$]
Completeness to theta $=29.63°$	99.2%
Absorption correction	Semi-empirical from equivalents
Max. and min. transmission	0.518 and 0.271
Refinement method	Full-matrix least-squares on F^2
Data/restraints/parameters	4082/0/163
Goodness-of-fit on F^2	0.996
Final R indices [I>2sigma(I)]	$R_1 = 0.0508, wR_2 = 0.0850$
R indices (all data)	$R_1 = 0.0990, wR_2 = 0.0968$
Largest diff. peak and hole	1.740 and -1.660 e Å^{-3}

$w = 1/[\sigma^2(F_o^2) + (0.0300P)^2 + 2.5P]$, where $P = (F_o^2 + 2F_c^2)/3$ using SHELXTL ver. 5.1 programs (*34*). A summary of crystal data, refinement details, and resultant refinement agreement factors are given in Table 5.

5.   Supplementary materials

Crystallographic data for the structural analysis have been deposited with the Cambridge Crystallographic Data Centre, CCDC No., [Cd(HL)I$_2$]: 745184. Copy of this information may be obtained free of charge from The Director, CCDC, 12 Union Road, Cambridge CB2 1EZ, UK (fax: 44-1223-336033; e-mail: deposit@ccdc.cam.ac.uk or http://www.ccdc.cam.ac.uk).

Acknowledgements

References

(1) Yazdanbakhsh, M.; Takjoo, R.; Frank, W.; Aghaei Kaju, A. *J. Coord. Chem.* **2009,** *62,* 3651–3660.
(2) Yazdanbakhsh, M.; Heravi, M.M.; Takjoo, R.; Frank, W. *Z. Anorg. Allg. Chem.* **2008,** *63,* 972–976.
(3) Lobana, T.S.; Sharma, R.; Bawa, G.; Khanna, S. *Coord. Chem. Rev.* **2009,** *253,* 977–1055.
(4) Mukesh Kumar, B.; Krishna, S.; Monika, S.; Nighat, F.; Ran Vir, S. *Transit. Met. Chem.* **2008,** *33,* 377–381.
(5) Chan, M.-H.E.; Crouse, K.A.; Tahir, M.I.M.; Rosli, R.; Umar-Tsafe, N.; Cowley, A.R. *Polyhedron* **2008,** *27,* 1141–1149.
(6) Seena, E.B.; Kurup, M.R.P. *Spectrochim. Acta A* **2008,** *69,* 726–732.
(7) Pedrido, R.; Bermejo, M.R.; Romero, M.J.; González-Noya, A.M.; Maneiro, M.; Fernández, M.I. *Inorg. Chem. Commun.* **2005,** *8,* 1036–1040.
(8) Novaković, S.B.; Fraisse, B.; Bogdanović, G.A.; Spasojević-de Biré, A. *Cryst. Growth Des.* **2007,** *7,* 191–195.
(9) Bermejoa, E.; Carballob, R.; Castiñeiras, A.; Domingueza, R.; Maichle-Mössmer, C.; Strähle, J.; West, D.X. *Polyhedron* **1999,** *18,* 3695–3702.
(10) Castiñeiras, A.; Garcia, I.; Bermejo, E.; West, D.X. *Polyhedron* **2000,** *19,* 1873–1880.
(11) West, D.X.; Swearingen, J.K.; Romack, T.J.; Billeh, I.S.; Jasinski, J.P.; Li, Y.; Staples, R.J. *J. Mol. Struct.* **2001,** *570,* 129–136.
(12) Ali, M.A.; Mirza, A.H.; Monsur, A.; Hossain, S.; Nazimuddin, M. *Polyhedron* **2001,** *20,* 1045–1052.
(13) Labisbal, E.; Sousa-Pedrares, A.; Castiñeiras, A.; Swearingen, J.K.; West, D.X. *Polyhedron* **2002,** *21,* 1553–1559.
(14) García, I.; Bermejo, E.; El Sawaf, A.K.; Castiñeiras, A.; West, D.X. *Polyhedron* **2002,** *21,* 729–737.
(15) Bermejo, E.; Castiñeiras, A.; Fostiak, L.M.; Santos, I.G.; Swearingen, J.K.; West, D.X. *Polyhedron* **2004,** *23,* 2303–2313.
(16) Rapheal, P.F.; Manoj, E.; Prathapachandra Kurup, M.R. *Polyhedron* **2007,** *26,* 818–828.
(17) Suni, V.; Prathapachandra Kurup, M.R.; Nethaji, M. *Polyhedron* **2007,** *26,* 5203–5209.
(18) Suni, V.; Prathapachandra Kurup, M.R.; Nethaji, M. *Spectrochim. Acta A* **2006,** *63,* 174–181.
(19) Fostiak, L.M.; García, I.; Swearingen, J.K.; Bermejo, E.; Castiñeiras, A.; West, D.X. *Polyhedron* **2003,** *22,* 83–92.
(20) Gómez-Saiz, P.; Gil-García, R.; Maestro, M.A.; Pizarro, J.L.; Arriortua, M.I.; Lezama, L.; Rojo, T.; González-Álvarez, M.; Borrás, J.; García-Tojal, J. *J. Inorg. Biochem.* **2008,** *102,* 1910–1920.
(21) Latheef, L.; Kurup, M.R.P. *Spectrochim. Acta A* **2008,** *70,* 86–93.
(22) John, R.P.; Sreekanth, A.; Prathapachandra Kurup, M.R.; Mobin, S.M. *Polyhedron* **2002,** *21,* 2515–2521.
(23) Qing, Y.; Hua, D.J.; Gang, Z.L.; Qing, Z.X.; Dong, B.H.; Hong, L. *J. Mol. Struct.* **2006,** *794,* 71–76.
(24) Sau, D.K.; Butcher, R.J.; Chaudhuri, S.; Saha, N. *Polyhedron* **2004,** *23,* 5–14.
(25) Bermejo, E.; Castiñeiras, A.; García, I.; West, D.X. *Polyhedron* **2003,** *22,* 1147–1154.
(26) Philip, V.; Suni, V.; Prathapachandra Kurup, M.R.; Nethaji, M. *Polyhedron* **2005,** *24,* 1133–1142.
(27) Joseph, M.; Suni, V.; Prathapachandra Kurup, M.R.; Nethaji, M.; Kishore, A.; Bhat, S.G. *Polyhedron* **2004,** *23,* 3069–3080.
(28) Castiñeiras, A.; Carballo, R.; Pérez, T. *Polyhedron* **2001,** *20,* 441–448.
(29) Addison, A.; Rao, T.; Reedjik, J.; Van Rijn, J.; Verschoor, G. *J. Chem. Soc. Dalton Trans.* **1984,** 1349–1356.
(30) Li, Q.-X.; Tang, H.-A.; Li, Y.-Z.; Wang, M.; Wang, L.-F.; Xia, C.-G. *J. Inorg. Biochem.* **2000,** *78,* 167–174.
(31) Tarafder, M.T.H.; Chew, K.-B.; Crouse, K.A.; Ali, A.M.; Yamin, B.M.; Fun, H.K. *Polyhedron* **2002,** *21,* 2683–2690.
(32) Blessing, R.H. *Acta. Crystallogr. Sect. A* **1995,** *51,* 33–38.
(33) Sheldrick, G.M. *Acta. Crystallogr. Sect. A* **1990,** *46,* 467–473.
(34) Sheldrick, G.M. *SHELX-97, SHELXS97*: University of Gottingen: Germany, 1997.